Available online at www.sciencedirect.com
ScienceDirect
Biochemical and Biophysical Research Communications 348 (2006) 47–55
BBRC
www.elsevier.com/locate/ybbrc

Identification of a new *in vivo* phosphorylation site in the cytoplasmic carboxyl terminus of EBV-LMP1 by tandem mass spectrometry ☆

Kun-Yi Chien [a,b], Yu-Sun Chang [b], Jau-Song Yu [a,b], Lin-Wen Fan [d], Chien-Wei Lee [c], Lang-Ming Chi [d,*]

[a] *Department of Biochemistry and Molecular Biology, Chang Gung University, Kwei-shan, Tao-Yuan, Taiwan*
[b] *Graduate Institute of Basic Medical Sciences, Chang Gung University, Kwei-shan, Tao-Yuan, Taiwan*
[c] *Molecular Medicine Research Center, Chang Gung University, Kwei-shan, Tao-Yuan, Taiwan*
[d] *Department of Medical Research and Development, Chang Gung Memorial Hospital, Lin-ko, Taiwan, ROC*

Received 24 June 2006
Available online 12 July 2006

Abstract

Latent membrane protein 1 (LMP1), an oncogenic protein encoded by Epstein–Barr virus (EBV), has been verified to be phosphorylated *in vitro* by protein casein kinase 2 (CK2). In this study, we characterized the phosphorylation of the carboxyl terminus of LMP1 fused with glutathione-*S*-transferase (GST-LMP1c) and the FLAG-epitope-tagged LMP1 (F-LMP1) proteins expressed in HEK293T cells. Using a combination of chemical modification and tandem mass spectrometry, we detected the phosphorylation of a tryptic peptide, 191–223 amino acids, in both GST-LMP1c catalysed by CK2 and F-LMP1-expressing cell lines. Serine residues at positions 211 and 215 were determined to be the substrates of CK2 *in vitro*. Most importantly, the S215 phosphorylation was also detected in F-LMP1-expressing human cell lines. The phosphorylation of S215, which is located in the carboxyl-terminus activation region 1 of LMP1, provides a new insight for investigating the role and modulation of the phosphorylation of LMP1.

Keywords: Phosphorylation; Latent membrane protein 1; Mass spectrometry

Latent membrane protein 1 (LMP1) is an Epstein–Barr virus (EBV)-encoded oncogenic protein that is expressed in viral latent infection status. It plays a critical role in the malignancy of nasopharyngeal carcinoma and EBV-associated lymphoma [1–3]. In EBV-infected or LMP1-gene transfected cells, LMP1 is expressed as an integral membrane protein comprising three structural regions, including the cytoplasmic amino terminus, transmembrane region, and cytoplasmic carboxyl terminus. Similar to most of the cellular receptors, the activation of LMP1 is regulated by molecular aggregation and post-translational modification [4–6]. The oligomerization and activation of LMP1 results from hydrophobic interactions between transmembrane regions and is independent of a ligand. Phosphorylation—one of the most important post-translational modifications—of LMP1 has been studied in various LMP1-expressing cells [7]. Using mutants of LMP1 as study materials and analytical techniques such as radio-isotopic labelling and two-dimensional gel electrophoresis, the existence of several phosphorylated forms of LMP1 has been confirmed. Although two amino acid residues, namely, S313 and T324, have been implicated as the major phosphorylation sites of LMP1 [7], the kinase responsible for the phosphorylation of LMP1 and the exact phosphorylation sites in cells remain ambiguous.

Currently, tandem mass spectrometry-based methods have emerged as powerful and preferred tools for the

☆ *Abbreviations:* CTAR1, carboxyl-terminal activation region 1; EBV, Epstein–Barr virus; LMP1, latent membrane protein 1; MALDI-TOF MS, matrix-assisted laser desorption/ionization-time of flight mass spectrometry; CK2, protein casein kinase 2; TBB, 4,5,6,7-tetrabromobenzimidazole.

* Corresponding author. Fax: +888 3 2118683.
E-mail address: lmchi@mail.cgu.edu.tw (L.-M. Chi).

0006-291X/$ - see front matter © 2006 Elsevier Inc. All rights reserved.
doi:10.1016/j.bbrc.2006.06.188

analysis of protein phosphorylation because of their high sensitivity and accuracy as well as the absence of hazardous radio-isotopic labelling [8,9]. However, low abundance, ionization suppression of the phosphate moiety, and the metastable loss of HPO_3 (−80) and H_3PO_4 (−98) from the parent ions [10–13] are the factors that challenge the specific characterization of phosphorylation sites by using tandem mass spectrometry. Therefore, various techniques have been developed to overcome these limitations [14–17]. Among these techniques, immobilized metal affinity chromatography (IMAC) is one of the most popular techniques to enrich phosphopeptides or phosphoproteins [18–20]. However, acidic biomolecules interfere with the binding capacity and efficiency of IMAC, thereby restricting its utility [21–24].

The cytoplasmic carboxyl terminus of LMP1, which is rich in acidic residues, is the only possible region that can be phosphorylated *in vivo*. Previously, using an *in vitro* kinase assay, we demonstrated that several serine residues in this region could be the targets for recombinant and cellular CK2 [25]. In the present study, we investigated the exact phosphorylation sites of recombinant LMP1 catalysed by CK2 *in vitro* and the phosphorylation sites of LMP1 expressed in human cells by tandem mass spectrometry. Our results clearly showed that S211 and S215 that are located in the carboxyl-terminus activating region 1 (CTAR1) of LMP1 could be phosphorylated by CK2 *in vitro*. Most importantly, we demonstrated that S215 is the major phosphorylation site in CTAR1 of LMP1 expressed in human cell lines.

Materials and methods

Materials. Most of the chemicals were purchased from Sigma Chemical Co. (St. Louis, MO). The sequencing grade trypsin was obtained from Promega (Madison, WI). $ZipTip_{C18}$, a tip-type reverse-phase column, was from Millipore (Bedford, MA). The protease inhibitor cocktail was obtained from Roche. A SphereClone 5-μ SAX column was purchased from Phenomenex (Torrance, CA).

Phosphorylation of GST-LMP1c protein. The GST-LMP1 fusion proteins with the entire carboxyl-terminal portion of LMP1 (GST-LMP1c) were expressed and purified as described previously [25]. The purified GST-LMP1c protein (5–10 μg) was phosphorylated by 20–40 U CK2 (New England Biolabs, Beverly, MA) in a 30-μl phosphorylation buffer (100 mM KCl, 1 mM DTT, 20 mM $MgCl_2$, 200 mM ATP, and 20 mM Tris, pH 7.5) at 30 °C for specific time intervals, as indicated. The reaction was terminated by heating at 95 °C for 5 min.

Construction and expression of FLAG-epitope-tagged LMP1 and its mutants. The full-length LMP1 gene in the pEGFP vector (a gift from Bill Sugden, McArdle Laboratory for Cancer Research, Madison) was amplified using the primer pairs B+43 (5′ACTCAAGCTTATGGAAC ACGACCTTGAG3′) and L1-4 (5′CGCGGATCCTTAGTCATAGTA GCTTAG3′). The *Bam*HI and *Hin*dIII digest fragments of the amplicon were subcloned into the pCMV-FLAG2 vector (a gift from Zee-Fen Chang, Graduate Institute of Biochemistry and Molecular Biology, National Taiwan University, Taiwan) to generate FLAG-tagged LMP1 (F-LMP1). The mutants of F-LMP1, F-S211A, and F-S215A were generated by the overlapping PCR method using two primer pairs, S211A-F (5′CGATGATGCTGGCCATG3′) and S211A-R (5′CATGGCCAGCA TCATCG3′) for the F-S211A mutant, and S215A-F (5′TCTGGCCATG AAGAGGTATCTAACTC3′) and S215A-R (5′AGTTAGAGTCCTCT TCATGGCCAG3′) for the F-S215A mutant. The purified pCMV-FLAG2 plasmid with or without the LMP1 gene insert was transfected into 60% confluent human embryonic kidney 293T (HEK293T) cells by using the calcium phosphate precipitation method. The cells were maintained in Dulbecco's modified Eagle's medium (DMEM) supplemented with heat-inactivated 10% fetal bovine serum (FBS) and antibiotics (penicillin/streptomycin). After transfection for 24 h, the cells were harvested and lysed in Triton lysis buffer (100 mM NaCl, 50 mM Tris–HCl, 1% Triton X-100, 10 mM sodium fluoride, 1 mM sodium orthovanadate, and protease inhibitor cocktail).

Immunoprecipitation of F-LMP1 protein. The lysate containing 1 mg of total protein was pre-incubated with 50 μl of protein G–Sepharose beads (Amersham Pharmacia Biotech) at 4 °C for 1 h. After centrifugation, the supernatant was incubated with 30 μl of agarose beads conjugated with anti-FLAG M2 antibody at 4 °C overnight. The beads were then washed sequentially with 20 volumes of Triton lysis buffer, saline buffer (150 mM NaCl, 50 mM Tris–HCl, pH 7.5), and low-salt buffer (50 mM Tris, pH 7.5).

Fractionation of tryptic peptides. The phosphorylated or non-phosphorylated GST-LMP1c and the affinity-purified F-LMP1 were digested with trypsin (enzyme:substrate = 1:50 by weight) at 37 °C overnight. For phosphopeptide enrichment, the tryptic peptide mixture containing phosphopeptides was diluted five-fold with binding buffer (50 mM ammonium formate (AF) at pH 6.8 and 15% acetonitrile (ACN)) and then applied onto a laboratory-scale 10 μl-microtip column packed with an anion exchange resin—SphereClone 5-μ SAX (particle size, 5 μm; pore size, 80 Å). After washing with 40 μl of binding buffer, the bound peptides were eluted by a step gradient from 100 to 500 mM AF as indicated. The peptides were then desalted by $ZipTip_{C18}$ according to the manufacturer's instructions prior to MS analysis. For determining the relative amount of phosphorylated peptides in different samples (see Results section), the tryptic peptides were acidified with 1% trifluoroacetic acid (TFA) and directly fractionated in a 10 μl-microtip column packed with reverse-phase resin (LiChrosphere RP-18; particle size, 5 μm; Merck, Germany). After washing with 5% ACN/TFA solvent, the peptides were fractionated by a step-increased ACN gradient. The tCTAR1 and its phosphoryl derivatives eluted in 10–15% ACN/TFA solvent were collected.

β-Elimination/Michael addition. The β-elimination/Michael addition reaction was performed according to the method described by Knight et al. [26]. Briefly, the phosphopeptides were incubated in 0.2 N NaOH for 1 h at ambient temperature and then in 0.2 N β-mercaptoethylamine (βMEA) solution for another 2–4 h at 37 °C. The reaction was terminated by the addition of 10–20 volumes of 1% TFA. The acidified sample was desalted and concentrated using $ZipTip_{C18}$. Aminoethylcysteine-modified peptides were then analysed by matrix-assisted laser desorption/ionization-time of flight (MALDI-TOF) mass spectrometry.

MALDI-TOF mass spectrometric analysis. The MS and MS/MS spectra were performed in an Ultraflex MALDI-TOF instrument (Bruker Daltonic GmbH, Bremen, Germany) equipped with a nitrogen laser (337 nm). The peptide solution was spotted on the MALDI plate and then co-crystallized with 0.3 μl α-cyano-4-hydroxycinnamic acid (CHCA) matrix solution (2 mg/ml in 80% ACN and 0.1% TFA) containing internal peptide mass standards. The instrument was operated in the linear mode for phosphopeptide detection, in the reflectron mode to obtain an accurate m/z of peptides, and in the LIFT mode for tandem MS analysis. An accelerating voltage of 25 kV and a delay of 200 ns were used in both linear and reflectron mode analyses. Calibration of the instrument was performed internally with $[M+H]^+$ ions of bovine serum albumin (BSA) (161–167 and 421–433) and adrenocorticotropic hormones (18–39), respectively. In the TOF1 stage of the LIFT mode, all ions were accelerated by 8 kV under conditions to promote metastable fragmentation. After selection of jointly migrating parent and fragment ions in a timed ion gate, the ions were lifted by 19 kV to a high potential energy in the LIFT cell. After further acceleration of the fragment ions in the second ion source, their masses were simultaneously analysed in the reflector with high sensitivity. All the processed spectra were analysed using Bruker's BioTools™ and Mascot (Matrix Science Ltd, London, UK) software, combined with user-defined modified amino acids.

Results

Detection of the CK2-catalysed phosphorylation of GST-LMP1c by MALDI-TOF MS

GST-LMP1c containing the cytoplasmic carboxyl terminus of LMP1 was expressed in *Escherichia coli* and purified by glutathione affinity column chromatography as described previously [25]. The structural and amino acid sequences of GST-LMP1c are shown in Fig. 1. The amino acid sequence and the theoretical masses of tryptic peptides derived from the carboxyl terminus of LMP1 are summarized in Table 1. The three tryptic fragments were tentatively denoted as tCTAR1, tCTAR3, and tCTAR2, due to the similar amino acid sequence when compared with the well-defined functional domains, CTAR1 (a.a. 187–231), CTAR3 (a.a. 232–351), and CTAR2 (a.a. 352–386) of LMP1, respectively. For detecting the phosphopeptides, GST-LMP1c with or without CK2 treatment was digested with trypsin overnight at ambient temperature. Without further purification, the tryptic peptides were analysed by MALDI-TOF MS in the linear mode (Fig. 2A). The tCTAR1 peptide with an average mass at *m*/*z* 3676.55 was detected. Interestingly, the monophosphoryl-tCTAR1, which has a theoretical average mass at *m*/*z* 3756.55, appeared when the CK2-catalysed reaction time was increased (Fig. 2A). The signals in *m*/*z* 5450–5500 may be contributed by tCTAR2 and doublet-charged tCTAR3. However, the phosphorylated peptides of tCTAR2 and tCTAR3 could not be detected. Therefore, the peptide corresponding to the phosphorylated tCTAR1 was further examined.

The enrichment and aminoethylcysteine modification of phosphorylated tCTAR1

In order to investigate the phosphorylation sites of tCTAR1, the phosphopeptide was first enriched by an anion exchanger instead of the commonly used IMAC because of the presence of multiple acidic amino acids and histidine residues in this peptide. The tryptic peptide mixture was separated on a microtip column packed with a SAX anion exchanger. As shown in Fig. 2B, the ions with the same average mass as monophosphorylated tCTAR1 at *m*/*z* 3756.5 were detected in the 300–400 mM ammonium formate-eluted fractions.

Since there are six serine (S) and one threonine (T) residues in tCTAR1, the β-elimination/Michael addition reaction was performed to accurately identify the phos-

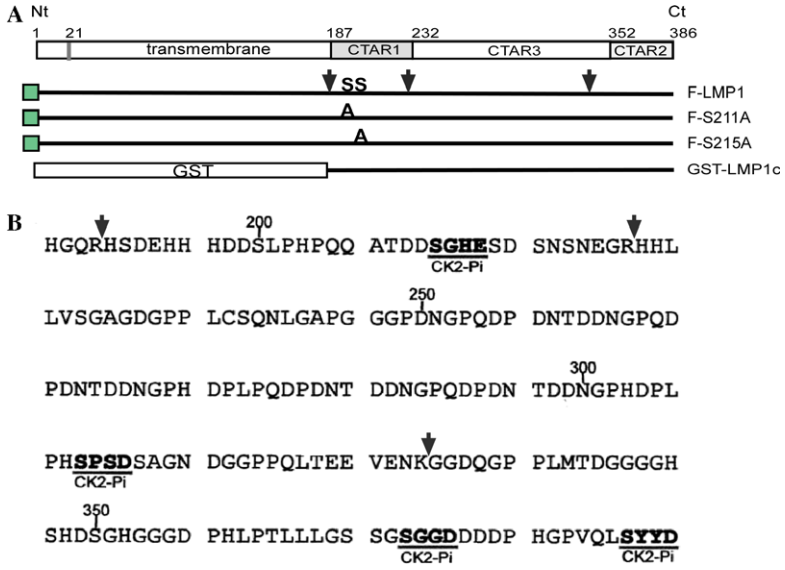

Fig. 1. The scheme of F-LMP1 and GST-LMP1c fusion proteins. (A) The structural and functional domains of full-length LMP1 are indicated. The polynucleotides encoding the full-length and carboxyl terminus (LMP1c) of LMP1 were fused to the 3′-end of FLAG (F-LMP1) and GST (GST-LMP1c), respectively. (B) The amino acid sequences of the cytoplasmic carboxyl terminus of LMP1. The trypsin digestion sites are indicated by arrows, and the CK2 recognition consensus sequences (CK2-Pi) are underlined.

Table 1
Theoretical monoisotopic and average masses of tryptic peptides derived from the cytoplasmic carboxyl terminus of LMP1

Peptide (position)	$[M+H]^+$		Amino acid sequence
	Average	Monoisotopic	
tCTAR1 (191–223)	3676.5536	3674.4743	HSDEHHHDDSLPHPQQATDD SGHESDSN SNEGR
tCTAR3 (224–330)	10936.0130	10929.6158	HHLLVSGAGDGPPLCSQNLGAPGGGPDNGP QDPDNTDDNGPQDPDNTDDNGPHDPLPQDP DNTDDNGPQDPDNTDDNGPH DPLPHSPSDS AGNDGGPPQLTEEVENK
tCTAR2 (331–386)	5452.6306	5449.3594	GGDQGPPLMTDGGGGHSHDSGHGGGDPHL PTLLLGSSGSG GDDDDPHGPVQLSYYD

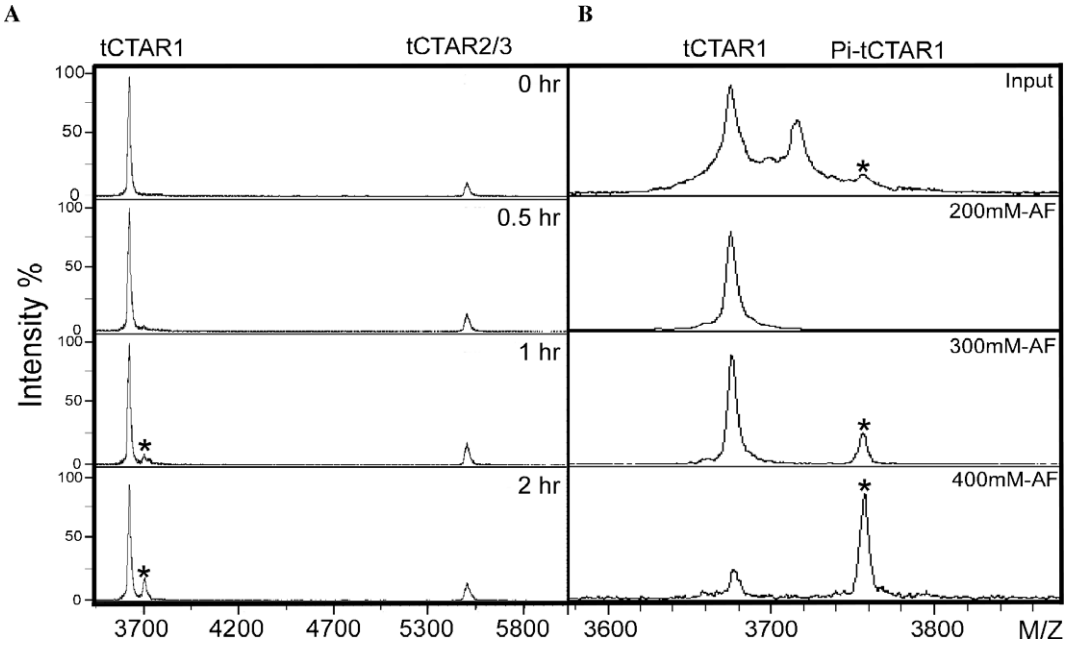

Fig. 2. tCTAR1 of GST-LMP1c phosphorylated by CK2. (A) Five micrograms of affinity-purified GST-LMP1c was incubated with 20 U CK2 for specific time, indicated. The reaction was terminated by heating at 95 °C for 5 min. The crude tryptic peptides (1/600) were spotted on the MALDI plate, co-crystallized with CHCA solution, and analysed by MALDI-TOF MS in the linear mode. The phosphopeptides are indicated by asterisks. (B) The tryptic peptides of 1 h-reaction product as shown in (A) and upper panel of (B) were further purified using a 5-μl bed volume SAX anion exchanger microtip column. The tCTAR1 peptide was eluted in the 200-mM AF fraction, and its phosphopeptides were enriched in the 300- and 400-mM AF fractions (pH 6.8). The mass spectra were acquired in the positive-ion linear mode.

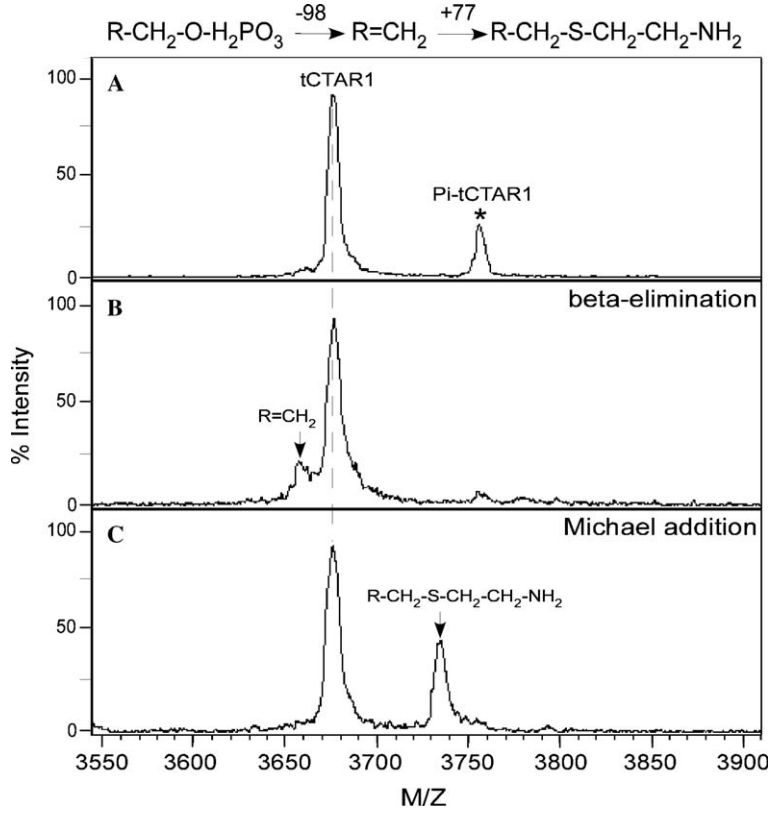

Fig. 3. The spectra of Pi-tCTAR1 and its chemical transformation derivates. The β-elimination/Michael addition reaction was performed for the monophosphopeptide of tCTAR1, as described in Materials and methods. (A) The 300-mM AF fraction before aminoethylcysteine modification. Pi-tCTAR1 is indicated by an asterisk. (B) The conversion of the phosphopeptide to a dehydroalanine-containing peptide under strong alkaline conditions. The peptide ion peak containing the dehydroalanine residue is indicated by an arrow. (C) The aminoethylcysteine derivative (indicated by an arrow) was finally obtained after the addition of βMEA. All the products were analysed by MALDI-TOF MS in the positive-ion linear mode. The scheme of the chemical transformation of phosphoserine to dehydroalanine (−98) and subsequently aminoethylcysteine (+77) is shown at the top of the figure.

phorylation sites. In the presence of NaOH and βMEA, the phosphoseryl and phosphothreonyl groups were converted to aminoethylcysteine and β-methylaminoethylcysteine, respectively. As shown in Figs. 2B and 3A, for the β-elimination/Michael addition reaction, the desalted ammonium formate-eluted fraction was treated with NaOH for 1 h and then incubated with βMEA for 4 h. The peptide with an average mass at *m*/*z* 3756.5 (Fig. 3A) was shifted to *m*/*z* 3658 (Fig. 3B) and then further shifted to *m*/*z* 3735 (Fig. 3C). All the peptide masses observed in these experiments were consistent with the theoretical masses of monophosphorylated tCTAR1 (Pi-tCTAR1) and its chemically modified derivates, which provide direct evidence that the ion at *m*/*z* 3756.5 should be Pi-tCTAR1. The phosphorylation sites of this phosphopeptide and its derivates were then analysed by MALDI-TOF/TOF tandem mass spectrometry (see below).

Identification of the phosphorylation sites of tCTAR1 catalysed by CK2

Three monoisotopic parent ions at *m*/*z* 3674.5, 3754.5, and 3735.5 that correspond to non-phosphorylated (tCTAR1), monophosphorylated (Pi-tCTAR1), and βMEA-tagged tCTAR1 (βMEA-tCTAR1), respectively, were selected for tandem mass analysis in the LIFT mode (Figs. 4A–C). Comparison of the product ion mass spectra revealed that the abundant fragment ion peak y7 appeared at the same *m*/*z* position in all spectra. The mass of the y13 fragment ion, another intense ion peak, was obviously different in these peptides. The peaks were observed at *m*/*z* 1375.4 for tCTAR1 (Fig. 4A), at *m*/*z* 1357.53 for Pi-tCTAR1 (Fig. 4B), and at *m*/*z* 1434.54 for βMEA-tCTAR1 (Fig. 4C). Therefore, the potential phosphorylation sites should be located between the y7 and y13 fragment ions. Based on the analysis of the ion peaks between the y7 and y13 fragment ions, we confirmed that S215 was the phosphorylation site.

To test whether there are multiple CK2-catalysed phosphorylation sites in tCTAR1, GST-LMP1c was phosphorylated by a higher amount of CK2 for a longer time (more than 4 h), and an aminoethylcysteine-modified peptide of potential diphosphorylated tCTAR1 (di-βMEA-tCTAR1) was prepared as described previously (Fig. 5A and B). The parent ion with monoisotopic mass at *m*/*z* 3794.5 that corresponded to di-βMEA-tagged peptide (di-βMEA-tCTAR1) was selected and reanalysed in the LIFT mode. In addition to S215, S211 was determined as the other residue that is phosphorylated by CK2, as shown in Figs. 5C and D.

Identification of the in vivo phosphorylation sites of tCTAR1

To examine if the CK2-catalysed S211 and S215 phosphorylations could occur *in vivo*, the phosphorylation of tCTAR1 in human cells was also analysed. The FLAG-

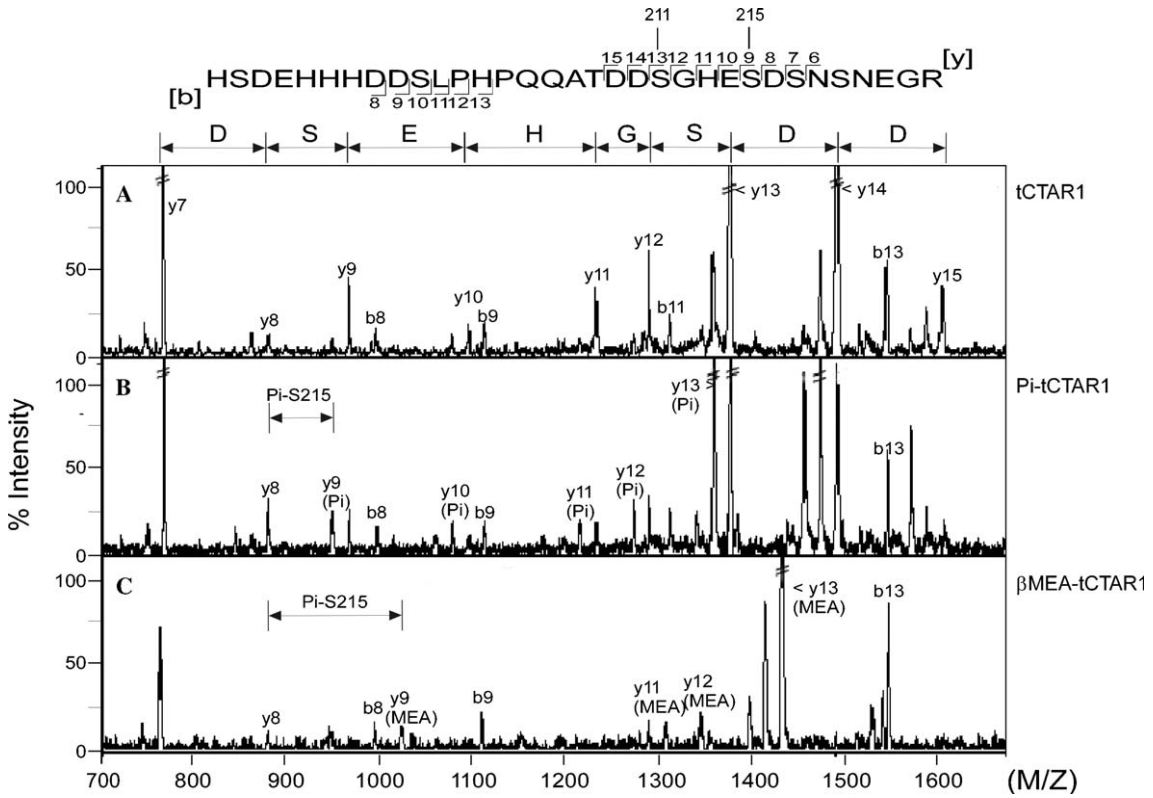

Fig. 4. MALDI-TOF MS/MS spectra of tCTAR1 and its derivatives. The phosphorylation site of tCTAR1 purified from tryptic GST-LMP1c mixture was analysed. The MS/MS spectra of monoisotopic mass (A) at *m*/*z* 3674.8, tCTAR1; (B) at *m*/*z* 3754.8, Pi-tCTAR1; and (C) at *m*/*z* 3735.8, βMEA-tCTAR1 were expanded from *m*/*z* 700 to 1700.

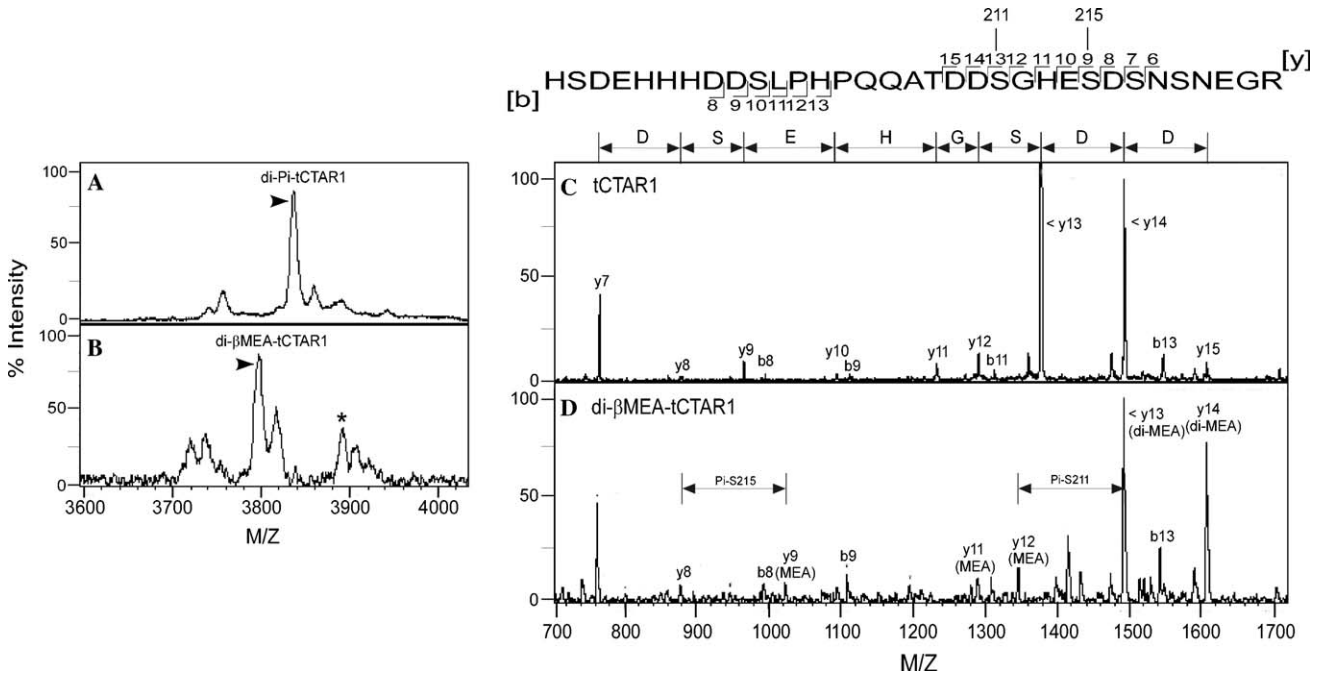

Fig. 5. MALDI-TOF MS and MS/MS spectra of double phosphorylated tCTAR1 and its derivatives. (A) The double phosphorylation form of tCTAR1 purified from the tryptic GST-LMP1c mixture was enriched and analysed by MALDI-TOF mass spectrometry, as shown in Fig. 2B. (B) The linear mode MS spectra of the β-elimination/Michael addition reaction products of di-Pi-tCTAR1. The products of β-elimination reaction are indicated by asterisk. (C,D) The MS/MS spectra of monoisotopic mass (C) at *m*/*z* 3674.8, tCTAR1 as shown in Fig. 4A and (D) at *m*/*z* 3794.09, di-βMEA-tCTAR1.

tagged full-length LMP1 (F-LMP1) protein was expressed in HEK293T cells, affinity purified by anti-FLAG M2 beads, and resolved in a 10% SDS–PAGE gel (Fig. 6A, lane 3). The purified F-LMP1 was then trypsinized in-solution status because the three tryptic fragments in the cytoplasmic carboxyl terminus were too large to be extracted efficiently when in-gel digestion was performed. After trypsinization, tCTAR1 was separated from other peptides by an RP-18 microtip column. As shown in the upper panel of Fig. 6B, the peptides with average masses at *m*/*z* 3676.5 and 3756.5 corresponding to tCTAR1 and Pi-tCTAR1, respectively, were observed. However, the signals for tCTAR2 and tCTAR3 at the theoretical average mass at *m*/*z* 10936 and 5452.6, respectively, could not be clearly distinguished probably due to the interference from other proteins co-purified during immunoprecipitation (data not shown). This result indicates that tCTAR1 is phosphorylated when LMP1 is expressed in cells. Detailed analysis of the zoom-in fragment ion spectra of the parent ions at *m*/*z* 3674.5 and 3754.5 derived from tCTAR1 of wild-type LMP1 clearly indicates the existence of one phosphorylated residue between the y8 and y9 ions, i.e., S215 (see Figs. 6C and D for comparison). For understanding the role of S211 and S215 in tCTAR1 phosphorylation *in vivo*, the F-LMP1 mutants in which serine was replaced with alanine (F-S211A and F-S215A) were generated and expressed in HEK293T cells. The tCTAR1 peptides of F-S211A and F-S215A ($tCTAR1^{S211A}$ and $tCTAR1^{S215A}$, respectively) were purified as described previously. Interestingly, the potential monophosphoryl tCTAR1 peak at average *m*/*z* 3756 disappeared when serine was replaced with alanine at position 215 (Fig. 6B, lower panel). However, the phosphopeptide signal was still detectable in the F-S211A mutant. Comparison of the fragment ion spectra of the parent ions at *m*/*z* 3658.5 and 3738.5 corresponding to $tCTAR1^{S211A}$ and $Pi\text{-}tCTAR1^{S211A}$, respectively, confirmed the mutation of S211 and enabled the detection of the phosphorylation of S215 in the F-S211A protein (Figs. 6E and F). Taken together, these findings indicate that S215 is the major *in vivo* phosphorylation site of tCTAR1 in human cells.

Discussion

The functional domain, CTAR1, of LMP1 has been proposed to be phosphorylated or regulated by phosphorylation [27–29]. In our study, we demonstrated CTAR1 phosphorylation in LMP1-expressing human cell line. A novel phosphorylation site, namely S215, was characterized as the major phosphorylation residue. To specifically identify S215 as the phosphorylation site in the monophosphorylation status, the TOF/TOF spectra of tCTAR1 peptides with or without phosphorylation were compared (Figs. 4A and B; Figs. 6C and D). As shown in Fig. 4, the signals of fragment ions between the y7 and y13 ions are critical for determining the phosphorylation sites. However, the peaks within this region are too weak to accurately determine the phosphorylated residues—S211 or S215. For reducing the complexity of spectra caused by the neu-

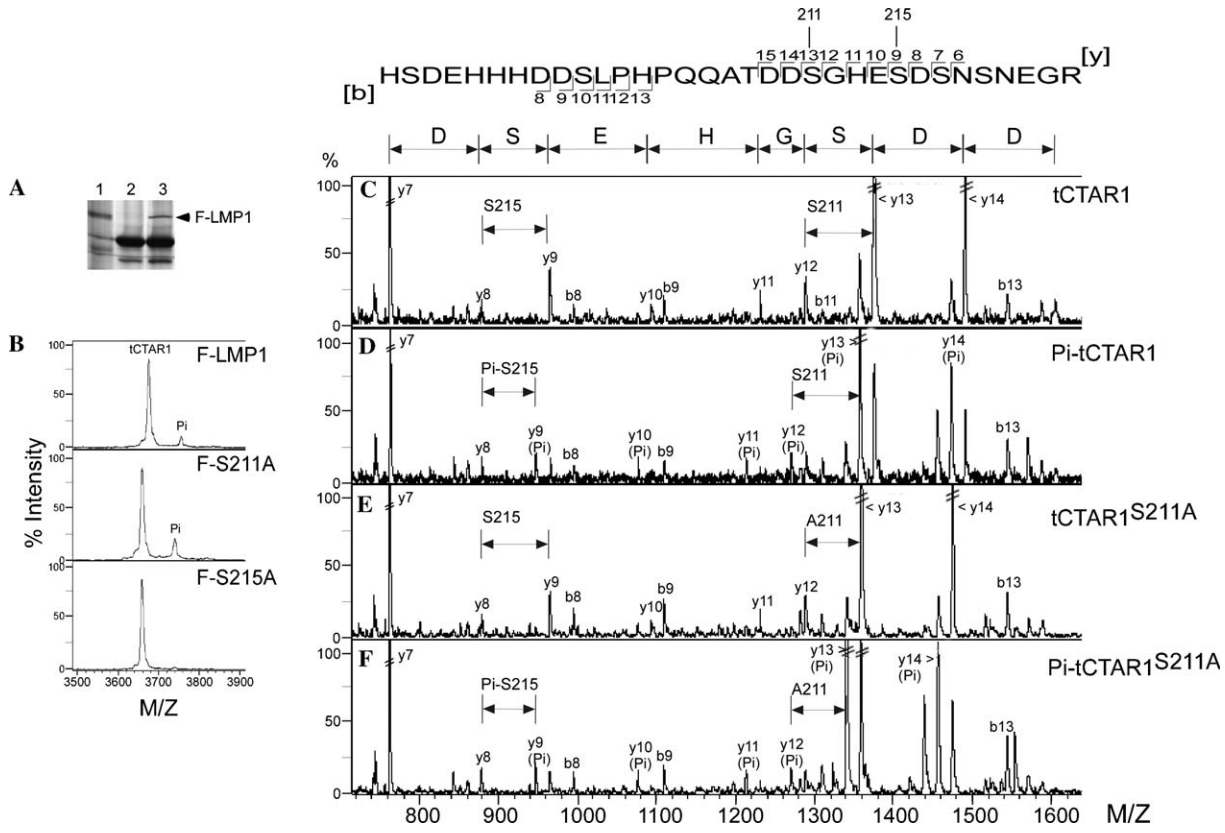

Fig. 6. Identification of the *in vivo* tCTAR1 phosphorylation site of F-LMP1 by MALDI-TOF MS/MS analysis. (A) The F-LMP1 expressed in HEK293T cells was immunoprecipitated using anti-FLAG M2 antibody, resolved in a 10% SDS–PAGE gel, and detected by silver staining. Lane 1: protein marker (M12, Invitrogen); lanes 2 and 3: the IP-purified protein from the lysate of HEK293T cells transfected with pCMV-FLAG2 (lane 2) or pCMV-F-LMP1 (lane 3). The F-LMP1 protein is indicated by an arrow. (B) The MS spectra of tCTAR1 peptides of F-LMP1, F-S211A, and F-S215A. The tCTAR1 fraction was purified from the tryptic peptide mixture using a reverse phase RP-18 microcolumn. The 12–16% ACN/TFA-eluted fraction was collected and analysed by MALDI-TOF MS in the positive-ion linear mode. (C–F) The TOF/TOF MS spectra of monoisotopic mass at *m/z* 3674.5, tCTAR1 (C); at *m/z* 3754.8, Pi-tCTAR1 (D); at *m/z* 3658.5, tCTAR1^{S211A} (E); and at *m/z* 3738.5, Pi-tCTAR1^{S211A} (F) were expanded from *m/z* 700 to 1650.

tral loss of the phosphopeptide, phosphoserine or phosphothreonine was chemically tagged with βMEA by β-elimination/Michael addition reaction. Comparison of the results of fragment ions of non-phosphorylated (Fig. 4A), phosphorylated (Fig. 4B), and chemically tagged (Fig. 4C) tCTAR1 parent ions revealed that S215 was phosphorylated by CK2 during monophosphorylation reaction. Based on this method, the phosphoryl S215 of LMP1 was also determined in human HEK293T cells (Figs. 6C and D).

To examine the possibility that the phosphorylation of S211 could be observed in monophosphorylated peptide, we evaluated the tiny peaks around the y9 ions. The other critical ions from b21 to b24 were also examined (data not shown). However, the S211 phosphorylation in the monophosphorylation status could not be detected. Several possibilities exist in this regard. First, the phosphorylation of S211 may occur only when S215 is phosphorylated. Second, the LMP1 protein becomes unstable when S211 is phosphorylated. Third, the phosphorylation of S211 is stimulated under certain physiological conditions. Fourth, the population of Pi-tCTAR1^{S211A} is too small to be detected. In fact, the phosphorylation of S211 was only observed when tCTAR1 was in the double phosphorylation state in our study (Fig. 5). The replacement of S215 with Ala—a residue that cannot be phosphorylated—dramatically affected the phosphorylation of tCTAR1 (Fig. 6B). These findings indicate that the phosphorylation of S211 may be dependent on S215. In contrast, the comparison of the relative mass signal of Pi-tCTAR1^{S211A} to that of Pi-tCTAR1 (Fig. 6B) indicates that the phosphorylation of S215 may be independent of S211. However, we cannot rule out these possibilities. In future studies, the extent of tCTAR1 phosphorylation in LMP1 and its mutants will be explored by the stable isotope labelling with amino acids in cell culture (SILAC) [30,31].

Although S313 and T324 have been characterized as the phosphorylation residues, the multiple phosphorylation status and the S313- and T324-independent ubiquitination of LMP1 indicate that another phosphorylation site in addition to S313 and T324 exist [7,29,32]. This study revealed a novel phosphorylation site S215 located in the CTAR1 function domain *in vivo* and the CK2-catalysed residues *in vitro*.

CK2 is ubiquitously expressed in eukaryotic cells as a constitutively active S/T kinase. It targets hundreds of

cellular and viral proteins [33–35]. The phosphoacceptor sites of CK2 are specified by multiple acidic residues downstream from the phosphorylable amino acid [33,36]. The acidic side chain at position $n + 3$ plays the most prominent role in susceptibility to CK2 phosphorylation [37]. Based on the typical substrate consensus sequence of CK2, S211 matches the request that with the acidic amino acids in the downstream. Although there is no acidic residue at position $n + 3$, S215—similar to S392 in p53—located in a sequence surrounded by acidic residues at both sides could be recognized by CK2 [38,39].

LMP1 was verified to be an oncoprotein that regulates cell division, proliferation, and apoptosis. CTAR1—one of the essential regions of LMP1—modulates cellular functions by interacting with cellular proteins and modulating the protein stability [27,28,40,41]. To the best of our knowledge, this study is the first to report the phosphorylation of CTAR1 *in vivo* and to prove that S215 is the phosphorylation site. The modulation and function of S215 phosphorylation will be investigated in future studies.

Acknowledgments

The authors appreciate the facilities provided by the Proteomics Core Laboratory and Molecular Medicine Research Center at Chang Gung University, Taiwan. This work was supported by the National Science Council (NSC92-2314-B-264-002 and NSC93-2320-B-182-012) and by grants (CMRPD140041 and CMRPG340141) from Chang Gung University and Memorial Hospital, Taiwan, the Republic of China.

References

[1] U. Dirmeier, R. Hoffmann, E. Kilger, U. Schultheiss, C. Briseno, O. Gires, A. Kieser, D. Eick, B. Sugden, W. Hammerschmidt, Latent membrane protein 1 of Epstein–Barr virus coordinately regulates proliferation with control of apoptosis, Oncogene 24 (2005) 1711–1717.
[2] I. Najjar, F. Baran-Marszak, C.C. Le, C. Laguillier, O. Schischmanoff, I. Youlyouz-Marfak, M. Schlee, G.W. Bornkamm, M. Raphael, J. Feuillard, R. Fagard, Latent membrane protein 1 regulates STAT1 through NF-kappaB-dependent interferon secretion in Epstein–Barr virus-immortalized B cells, J. Virol. 79 (2005) 4936–4943.
[3] J.S. Burgos, Involvement of the Epstein–Barr virus in the nasopharyngeal carcinoma pathogenesis, Med. Oncol. 22 (2005) 113–121.
[4] W.F. Coffin III, T.R. Geiger, J.M. Martin, Transmembrane domains 1 and 2 of the latent membrane protein 1 of Epstein–Barr virus contain a lipid raft targeting signal and play a critical role in cytostasis, J. Virol. 77 (2003) 3749–3758.
[5] N. Lam, B. Sugden, LMP1, a viral relative of the TNF receptor family, signals principally from intracellular compartments, EMBO J. 22 (2003) 3027–3038.
[6] A. Kaykas, K. Worringer, B. Sugden, LMP-1's transmembrane domains encode multiple functions required for LMP-1's efficient signaling, J. Virol. 76 (2002) 11551–11560.
[7] R.K. Moorthy, D.A. Thorley-Lawson, Biochemical, genetic, and functional analyses of the phosphorylation sites on the Epstein–Barr virus-encoded oncogenic latent membrane protein LMP-1, J. Virol. 67 (1993) 2637–2645.
[8] B.A. Garcia, J. Shabanowitz, D.F. Hunt, Analysis of protein phosphorylation by mass spectrometry, Methods 35 (2005) 256–264.
[9] M. Mann, S.E. Ong, M. Gronborg, H. Steen, O.N. Jensen, A. Pandey, Analysis of protein phosphorylation using mass spectrometry: deciphering the phosphoproteome, Trends Biotechnol. 20 (2002) 261–268.
[10] H. Zhou, J.D. Watts, R. Aebersold, A systematic approach to the analysis of protein phosphorylation, Nat. Biotechnol. 19 (2001) 375–378.
[11] Y. Oda, T. Nagasu, B.T. Chait, Enrichment analysis of phosphorylated proteins as a tool for probing the phosphoproteome, Nat. Biotechnol. 19 (2001) 379–382.
[12] E.C. Peters, A. Brock, S.B. Ficarro, Exploring the phosphoproteome with mass spectrometry, Mini Rev. Med. Chem. 4 (2004) 313–324.
[13] F. Meggio, L.A. Pinna, One-thousand-and-one substrates of protein kinase CK2? FASEB J. 17 (2003) 349–368.
[14] N. Imam-Sghiouar, R. Joubert-Caron, M. Caron, Application of metal-chelate affinity chromatography to the study of the phosphoproteome, Amino Acids 28 (2005) 105–109.
[15] J. Rush, A. Moritz, K.A. Lee, A. Guo, V.L. Goss, E.J. Spek, H. Zhang, X.M. Zha, R.D. Polakiewicz, M.J. Comb, Immunoaffinity profiling of tyrosine phosphorylation in cancer cells, Nat. Biotechnol. 23 (2005) 94–101.
[16] Y. Oda, T. Nagasu, B.T. Chait, Enrichment analysis of phosphorylated proteins as a tool for probing the phosphoproteome, Nat. Biotechnol. 19 (2001) 379–382.
[17] Y. Zhang, A. Wolf-Yadlin, P.L. Ross, D.J. Pappin, J. Rush, D.A. Lauffenburger, F.M. White, Time-resolved mass spectrometry of tyrosine phosphorylatiopn sites in the EGF receptor signaling network reveals dynamic modules, Mol. Cell. Proteomics (2005).
[18] E.E. Boeri, E. Bergatto, S. Cabodi, L. Silengo, G. Tarone, P. Defilippi, O.N. Jensen, Systematic analysis of the epidermal growth factor receptor by mass spectrometry reveals stimulation-dependent multisite phosphorylation, Mol. Cell. Proteomics 4 (2005) 1107–1121.
[19] Y.H. Ahn, E.J. Park, K. Cho, J.Y. Kim, S.H. Ha, S.H. Ryu, J.S. Yoo, Dynamic identification of phosphopeptides using immobilized metal ion affinity chromatography enrichment, subsequent partial beta-elimination/chemical tagging and matrix-assisted laser desorption/ionization mass spectrometric analysis, Rapid Commun. Mass Spectrom. 18 (2004) 2495–2501.
[20] A. Pandey, J.S. Andersen, M. Mann, Use of mass spectrometry to study signaling pathways, Sci. STKE 2000 (2000) L1.
[21] X. Wang, M.B. Goshe, E.J. Soderblom, B.S. Phinney, J.A. Kuchar, J. Li, T. Asami, S. Yoshida, S.C. Huber, S.D. Clouse, Identification and functional analysis of in vivo phosphorylation sites of the arabidopsis BRASSINOSTEROID-INSENSITIVE1 receptor kinase, Plant Cell (2005).
[22] X. Sun, J.F. Chiu, Q.Y. He, Application of immobilized metal affinity chromatography in proteomics, Expert Rev. Proteomics 2 (2005) 649–657.
[23] E.H. Seeley, L.D. Riggs, F.E. Regnier, Reduction of non-specific binding in Ga(III) immobilized metal affinity chromatography for phosphopeptides by using endoproteinase glu-C as the digestive enzyme, J. Chromatogr. B Analyt. Technol. Biomed. Life Sci. 817 (2005) 81–88.
[24] V. Gaberc-Porekar, V. Menart, Perspectives of immobilized-metal affinity chromatography, J. Biochem. Biophys. Methods 49 (2001) 335–360.
[25] L.M. Chi, J.S. Yu, Y.S. Chang, Identification of protein kinase CK2 as a potent kinase of Epstein–Barr virus latent membrane protein 1, Biochem. Biophys. Res. Commun. 294 (2002) 586–591.
[26] Z.A. Knight, B. Schilling, R.H. Row, D.M. Kenski, B.W. Gibson, K.M. Shokat, Phosphospecific proteolysis for mapping sites of protein phosphorylation, Nat. Biotechnol. 21 (2003) 1047–1054.
[27] W. Tang, O.A. Pavlish, V.S. Spiegelman, A.A. Parkhitko, S.Y. Fuchs, Interaction of Epstein–Barr virus latent membrane protein 1 with SCFHOS/beta-TrCP E3 ubiquitin ligase regulates extent of NF-kappaB activation, J. Biol. Chem. 278 (2003) 48942–48949.
[28] S. Rothenberger, K. Burns, M. Rousseaux, J. Tschopp, C. Bron, Ubiquitination of the Epstein–Barr virus-encoded latent membrane

protein 1 depends on the integrity of the TRAF binding site, Oncogene 22 (2003) 5614–5618.
[29] S. Aviel, G. Winberg, M. Massucci, A. Ciechanover, Degradation of the epstein–barr virus latent membrane protein 1 (LMP1) by the ubiquitin-proteasome pathway. Targeting via ubiquitination of the N-terminal residue, J. Biol. Chem. 275 (2000) 23491–23499.
[30] G. Zhang, D.S. Spellman, E.Y. Skolnik, T.A. Neubert, Quantitative phosphotyrosine proteomics of EphB2 signaling by stable isotope labeling with amino acids in cell culture (SILAC), J. Proteome Res. 5 (2006) 581–588.
[31] R. Amanchy, D.E. Kalume, A. Pandey, Stable isotope labeling with amino acids in cell culture (SILAC) for studying dynamics of protein abundance and posttranslational modifications, Sci. STKE 2005 (2005) l2.
[32] D. Liebowitz, R. Kopan, E. Fuchs, J. Sample, E. Kieff, An Epstein–Barr virus transforming protein associates with vimentin in lymphocytes, Mol. Cell. Biol. 7 (1987) 2299–2308.
[33] F. Meggio, L.A. Pinna, One-thousand-and-one substrates of protein kinase CK2? FASEB J. 17 (2003) 349–368.
[34] F. Meggio, O. Marin, M. Boschetti, S. Sarno, L.A. Pinna, HIV-1 Rev transactivator: a beta-subunit directed substrate and effector of protein kinase CK2, Mol. Cell. Biochem. 227 (2001) 145–151.
[35] A.S. El-Guindy, G. Miller, Phosphorylation of Epstein–Barr virus ZEBRA protein at its casein kinase 2 sites mediates its ability to repress activation of a viral lytic cycle late gene by Rta, J. Virol. 78 (2004) 7634–7644.
[36] L.A. Pinna, The raison d'etre of constitutively active protein kinases: the lesson of CK2, Acc. Chem. Res. 36 (2003) 378–384.
[37] L.A. Pinna, Casein kinase 2: an 'eminence grise' in cellular regulation? Biochim. Biophys. Acta 1054 (1990) 267–284.
[38] F. Meggio, O. Marin, L.A. Pinna, Substrate specificity of protein kinase CK2, Cell. Mol. Biol. Res. 40 (1994) 401–409.
[39] L. McKendrick, D. Milne, D. Meek, Protein kinase CK2-dependent regulation of p53 function: evidence that the phosphorylation status of the serine 386 (CK2) site of p53 is constitutive and stable, Mol. Cell. Biochem. 191 (1999) 187–199.
[40] B.A. Mainou, D.N. Everly Jr., N. Raab-Traub, Epstein–Barr virus latent membrane protein 1 CTAR1 mediates rodent and human fibroblast transformation through activation of PI3K, Oncogene 24 (2005) 6917–6924.
[41] P. Xie, G.A. Bishop, Roles of TNF receptor-associated factor 3 in signaling to B lymphocytes by carboxyl-terminal activating regions 1 and 2 of the EBV-encoded oncoprotein latent membrane protein 1, J. Immunol. 173 (2004) 5546–5555.